DUOX1 is required for airway epithelial cell migration and bronchiolar re-epithelialization following injury

Stefan H. Gorissen, Milena Hristova, Aida Habibovic, Lynne M. Sipsey, Page C. Spiess, Yvonne M.W. Janssen-Heininger, and Albert van der Vliet

ON-LINE DATA SUPPLEMENT

METHODS AND PROCEDURES

Isolation and Culture of Mouse Tracheal Epithelial Cells

Primary mouse tracheal epithelial (MTE) cells were isolated from C57BL/6 mice (Jackson Laboratory, Bar Harbor, ME) according to previously described procedures (1, 2). Briefly, tracheas were excised, filled with minimum essential medium (MEM) containing 0.1% protease 14 (Sigma-Aldrich, St. Louis, MO), and incubated overnight at 4°C. Tracheas were subsequently flushed with 5 mL of MEM containing 10% FBS, and detached cells were collected by centrifugation and cultured on rat tail collagen I gel (BD Biosciences, San Jose, CA) in DMEM/F12 media (Invitrogen, Grand Island, NY) containing 20 ng/mL cholera toxin (List Biological Laboratories, Campbell, CA), 10 ng/mL EGF (Calbiochem, San Diego, CA), 5 µg/mL insulin (Sigma), 5 µg/mL transferrin (Sigma), 100 nM dexamethasone (Sigma), 15 µg/mL bovine pituitary extract (Invitrogen), 2 mM L-glutamine, and 50 U/50 µg/mL Penicillin/Streptomycin (Pen/Strep) (Invitrogen). MTE cells were used in experiments at passages 2-4. MTE cells were also isolated from homozygous Tg $(CAT)^{+/+}$ mice (originally obtained from Dr. H. Van Remmen; University of Texas at San Antonio), which systematically overexpress the human *CAT* gene (3, 4).

Analysis of Epithelial Wound Closure and Cell Migration

MTE cells were seeded at 1×10^5 cells/cm^2 on collagen-coated 24-well plates (Becton Dickinson Labware, Bedford, MA) and grown until confluent, and subjected to scratch injury using a sterile pipette tip. Cells were rinsed with warm PBS after wounding to remove cellular debris and

placed in fresh media to monitor wound closure over 24 hrs, and wound areas were imaged at various time points using Image J software (NIH) for calculation of remaining wound areas. For a more quantitative analysis of epithelial cell migration driven by haptotaxis, MTE cells were seeded at 1×10^5 cells/well on 8-μm polycarbonate membrane inserts that were coated on the outside with 10 μg/ml fibronectin (Nunc) and incubated for 24 hrs. As controls, cells were seeded on inserts coated with 7.5% BSA instead of fibronectin. Non-migrated cells were removed with a cotton swab and remaining cells were stained with 0.1% crystal violet in 0.1 M sodium borate (pH 9.0)/ethanol (98%/2% v/v) and extracted with 10% acetic acid for quantitative analysis by absorbance at 562 nm (5).

RNAi Silencing of DUOX1 in MTE Cells

MTE cells were plated at 60-70% confluence and transfected with DUOX1 siRNA (Ambion) using DharmaFECT® transfection reagent (Dharmacon). Briefly, 0.5 μL of 2 DUOX1 siRNA targets (100 μM; Table I) were pre-mixed with 1.5 μL DharmaFECT reagent in 100 μL of media for 20-25 min and added to the MTE cells in 400 μL of media, and incubated overnight. Media was replaced the following day, and cells were used for experimentation after 3 days (72 hrs). As controls, similar transfections were performed with 1 μL of 100 μM non-target (NS) siRNA (Table I).

Naphthalene-Induced Airway Epithelial Injury

Airway epithelial injury was induced in C57BL/6 mice as described previously (6, 7). Briefly, mice received intraperitoneal injections of 20 mg/ml naphthalene (Sigma-Aldrich, St. Louis, MO) in corn oil (Mazola, Best Foods/CPC International, Englewood Cliffs, NJ), at a dose of 200

mg/kg, and vehicle control animals received equivalent volumes of corn oil. At 2, 7, and 14 days after naphthalene treatment (DPN), mice were euthanized with pentobarbital and tracheas were cannulated and lungs were collected and fixed with 1% PFA through the trachea at 30 cm of pressure for sectioning and immunohistochemical analysis. In addition, lung lobes were stored in RNAlater (Invitrogen) for subsequent RNA extraction or snap frozen in liquid nitrogen at stored -80°C for other biochemical analyses. All animal studies were approved by the University of Vermont Institutional Animal Care and Use Committee.

In Vivo siRNA Targeting of DUOX1

To address the importance of DUOX1 in epithelial repair following naphthalene-induced injury, DUOX1-targeted siRNA (Ambion) was administered in mice by oropharyngeal instillation under brief isofluorane anesthesia, prior to naphthalene injection. Two DUOX1 siRNA targets (Table I) were mixed in sterile PBS and instilled in a volume of 50-60 µL (35 µg/target sequence/mouse). Control animals received non-target NS siRNA (70 µg/mouse) similarly.

Western Blot Analysis

Frozen lung tissues were homogenized in cell lysis buffer (500 µL/lobe; Cell Signaling, Danvers, MA) supplemented with 1 mM phenylmethylsulfonyl fluoride (PMSF) (Sigma), briefly sonicated, and centrifuged (14,000 rpm; 10 min) to remove cell debris. Samples containing equal amounts of protein (20 µg; measured using BCA Protein Assay Kit; Pierce) were mixed with reducing Laemmli buffer (1.5% SDS, 10% glycerol, 62.5 mM Tris-HCl (pH 6.8), 0.0025% Bromophenol blue, and 2% β-mercaptoethanol) and separated by SDS-PAGE, followed by transfer onto nitrocellulose membranes for western blotting using primary antibodies (1:1000,

Cell Signaling) against phospho-EGFR (Y845), phospho-EGFR (Y1068), EGFR, phospho-ERK1/2, ERK1/2, phospho-Src (Tyr416), Src, phospho-STAT3 (Tyr705), STAT3, β-Actin (Sigma), and DUOX (kindly provided by F. Miot). Primary antibody binding was visualized using horseradish peroxidase (HRP)-linked secondary antibody (Cell Signaling) and enhanced chemiluminescence substrate (SuperSignal West Pico/Femto, Pierce). Densitometry of individual bands was performed using ImageJ software (NIH).

RT-PCR Analysis

Mouse tissues were homogenized in 1 mL TRIzol Reagent (Invitrogen) for 5 min, and insoluble material was removed by centrifugation at 8,000 rpm for 10 min at 4°C. Chloroform (200 µL) was added to the supernatant, which was then shaken vigorously, incubated for 3 minutes at room temperature, and centrifuged at 8,000 rpm for 10 minutes at 4°C. The upper RNA containing phenol-chloroform phase was used for subsequent RNA purification using RNeasy Mini Kit (Qiagen, Germantown, MD) according to manufactures instructions. RNA concentration was determined using a NanoDrop spectrophotometer (Thermo Scientific), and complementary DNA (cDNA) was synthesized from 1 µg of total RNA with $Oligo(dT)_{12-18}$ Primer and M-MLV Reverse Transcriptase (Invitrogen). In the PCR reaction, 5 µL of 1:10 diluted cDNA was amplified 33 times with Platinum Taq DNA Polymerase (Invitrogen) and appropriate primer sets (Table II). PCR products were visualized on 2% agarose gels stained with ethidium bromide, and gels were analyzed using the Gel Doc XR system and Quantity One 1-D analysis software (Bio-Rad Laboratories). Densitometry was performed using ImageJ software (NIH), and band densities were normalized to β-Actin. Alternatively, qPCR was

performed using SYBR Green PCR Supermix (BioRad) with appropriate primers (Table II) and normalized to GAPDH using the $\Delta\Delta C_T$ method.

Immunohistochemistry

PFA-fixed lung sections were paraffin-embedded, and 5-μm-thick sections were analyzed using antibodies against DUOX (kindly provided by Dr. Francoise Miot, Brussels, Belgium), rat α-CCSP (Millipore; 1:2000), and mouse anti-β-Tubulin IV (BioGenex; 1:200), or rabbit anti-phospho-STAT3 (Y705). Dual staining of CCSP and β-tubulin IV were performed using VECTOR® M.O.M Immunodetection kit (Vector Laboratories, Burlingame, CA), and primary antibodies were visualized using Alexa Fluor 555 Goat anti-rabbit (Invitrogen, 1:500) and streptavidin Alexa Fluor 647 conjugate (Invitrogen, 1:500), respectively, and sections were counterstained with DAPI (blue). Immunofluorescence analysis was performed using a Zeiss LSM 510 META confocal scanning laser microscope (Carl Zeiss Microimaging, Thornwood, NY) and images were analyzed using Metamorph® Microscopy Automation & Image Analysis Software (Molecular Devices).

SUPPLEMENTARY TABLE: RT-PCR Primer sequences used in this study.

RT-PCR primers:

mDUOX1:	F: caccsggaacggattgttct
	R: agcttctccgacatgatgct
mDUOX2	F: acggacatcgaagaaaccac
	R: cctgtcatacccgtcattca
β-actin	F: tctcagctgtggtggtgaag
	R: tgttaccaactgggacgaca

qPCR primers:

mDUOX1:	F: ATCTGGGTGACAAGGACTCA
	R: CAGACTCCTGTTCAGCACCT
GAPDH	F: CTGGAGAAACCTGCCAAGTA
	R: TGTTGCTGTAGCCGTATTCA

SUPPLEMENTARY FIGURES

Figure S1: Role of H_2O_2 in epithelial wound responses in MTE cells. (*A*) MTE cell monolayers were wounded and extent of wound closure was determined after 24 hrs in the absence or presence of catalase (2,000 U/ml) or exogenous H_2O_2 (1-100 μM). (*B*) Evaluation of wound closure rates in injured MTE cell monolayers in the presence of the H_2O_2 decomposition catalysts ebselen (10 μM) or EUK134 (50 μM). Mean S.E. of 4 replicates from 2 separate experiments are shown.

Figure S2: Role of endogenous catalase in MTE wound responses. MTE cells were isolated from either WT C57BL/6 mice and from Tg $(CAT)^{+/+}$ mice on a C57BL/6 background, and catalase expression was evaluated by Western blot analysis (*A*) and analysis of catalase activity (*B*). (*C*) Confluent monolayers of MTE cells from WT C57BL/6 mice and from Tg $(CAT)^{+/+}$ mice were scratch wounded and wound closure was monitored over 24 hrs. Mean ± S.E. from 4-6 replicates are shown.

Figure S3: Reversible epithelial injury in C57BL6 mice following naphthalene injection. (*A*) H&E staining of lung tissue sections showing the presence of exfoliated epithelial cells within the airway lumen 2 days after naphthalene instillation (2 DPN), which was not observed at 7 DPN or 14 DPN. Arrows: exfoliated cells; scale bars: 20 μm. (*B*) Ciliated cells become squamous and extend underneath the injured Clara cells before they are sloughed off into the airway lumen. Five μm thick sections were Immuno-labeled for CCSP (red) and β-Tubulin IV (green) and counterstained with DAPI (blue). (*a*) Control intact epithelium consists of Clara cells

(CCSP) and ciliated cells (β-Tubulin IV). (*b*) At 2 DPN ciliated cells become squamous and line the airways, while Clara cells are sloughed off. (*c*) At 7 DPN the airway epithelium is partially reconstructed, which is completed at 14 DPN (*d*). DPN: days post naphthalene, scale bars: 20 μm (top), 10 μm (bottom).

REFERENCES

E1. Wu R, Smith D. 1982. Continuous multiplication of rabbit tracheal epithelial cells in a defined, hormone-supplemented medium. *In Vitro* 18: 800-12

E2. Alcorn JF, Guala AS, van der Velden J, McElhinney B, Irvin CG, Davis RJ, Janssen-Heininger YM. 2008. Jun N-terminal kinase 1 regulates epithelial-to-mesenchymal transition induced by TGF-beta1. *J Cell Sci* 121: 1036-45

E3. Chen X, Liang H, Van Remmen H, Vijg J, Richardson A. 2004. Catalase transgenic mice: characterization and sensitivity to oxidative stress. *Arch Biochem Biophys* 422: 197-210

E4. Reynaert NL, Aesif SW, McGovern T, Brown A, Wouters EF, Irvin CG, Janssen-Heininger YM. 2007. Catalase overexpression fails to attenuate allergic airways disease in the mouse. *J Immunol* 178: 3814-21

E5. Bove PF, Hristova M, Wesley UV, Olson N, Lounsbury KM, van der Vliet A. 2008. Inflammatory levels of nitric oxide inhibit airway epithelial cell migration by inhibition of the kinase ERK1/2 and activation of hypoxia-inducible factor-1alpha. *J Biol Chem*

E6. Van Winkle LS, Isaac JM, Plopper CG. 1997. Distribution of epidermal growth factor receptor and ligands during bronchiolar epithelial repair from naphthalene-induced Clara cell injury in the mouse. *Am J Pathol* 151: 443-59

E7. Lawson GW, Van Winkle LS, Toskala E, Senior RM, Parks WC, Plopper CG. 2002. Mouse strain modulates the role of the ciliated cell in acute tracheobronchial airway injury-distal airways. *Am J Pathol* 160: 315-27

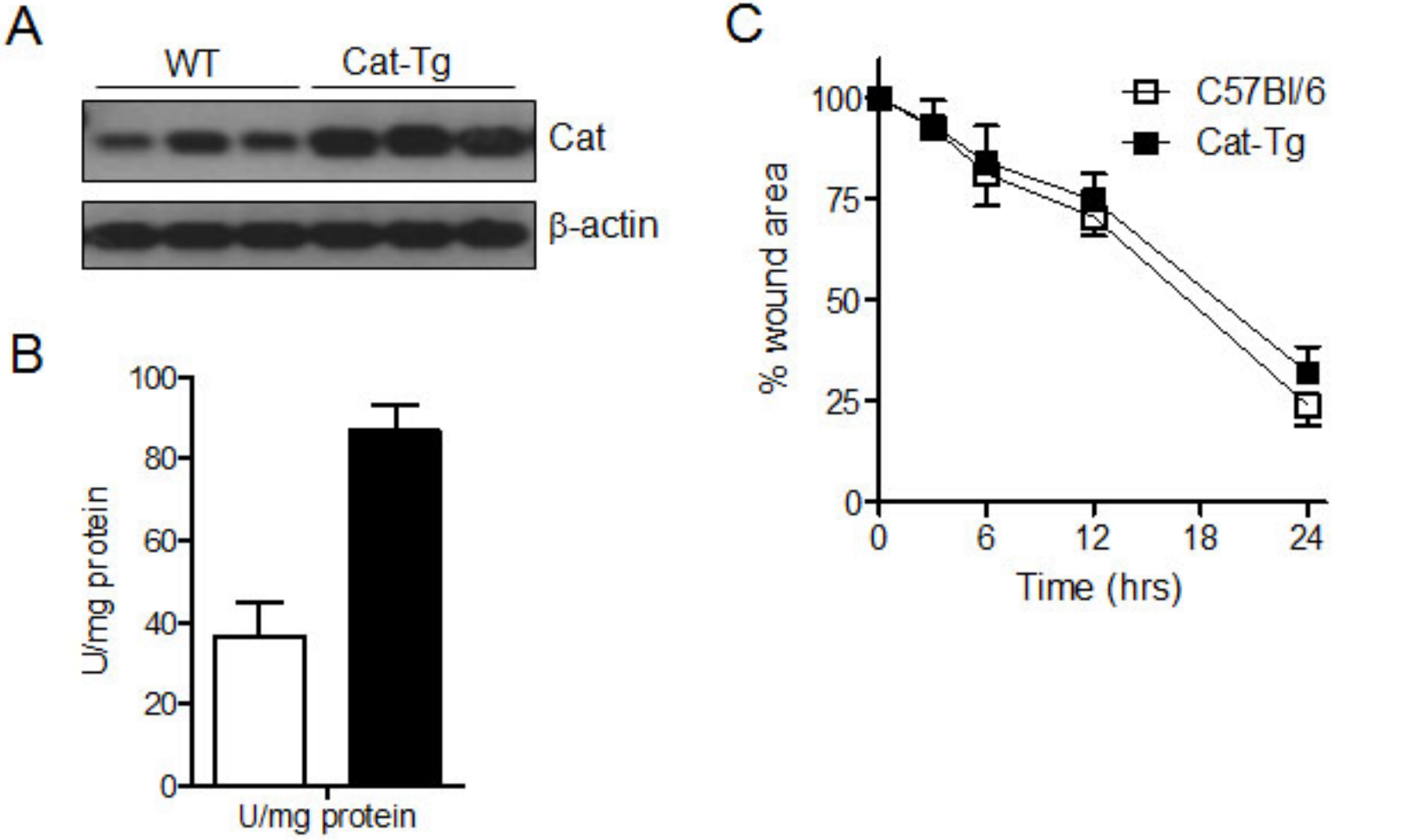
A
WT
Cat-Tg
Cat
β-actin
B
U/mg protein
100
80
60
40
20
0
U/mg protein
C
C57Bl/6
Cat-Tg
% wound area
100
75
50
25
0
0
6
12
18
24
Time (hrs)

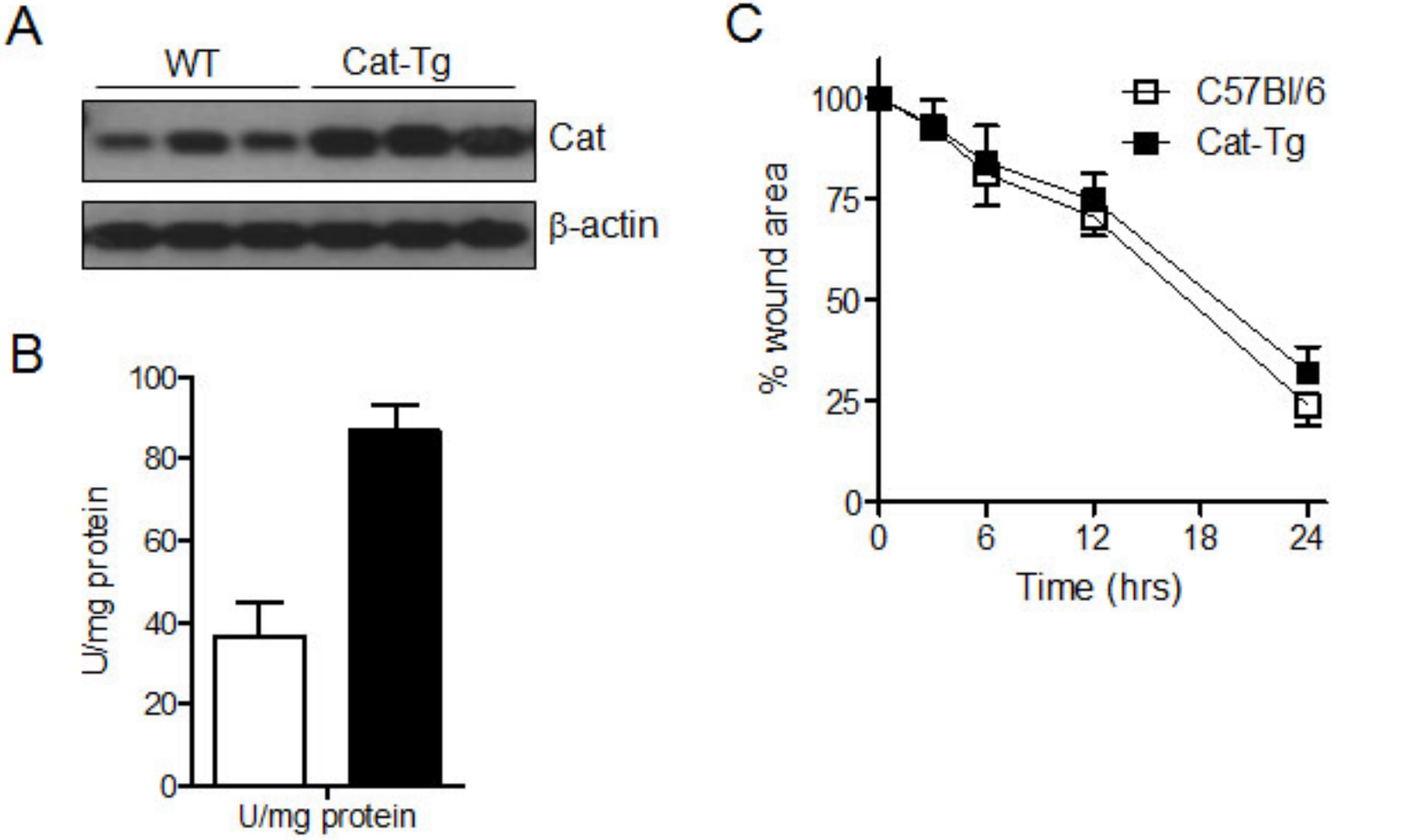
A
WT
Cat-Tg
Cat
β-actin
B
U/mg protein
100
80
60
40
20
0
U/mg protein
C
C57Bl/6
Cat-Tg
% wound area
100
75
50
25
0
0
6
12
18
24
Time (hrs)

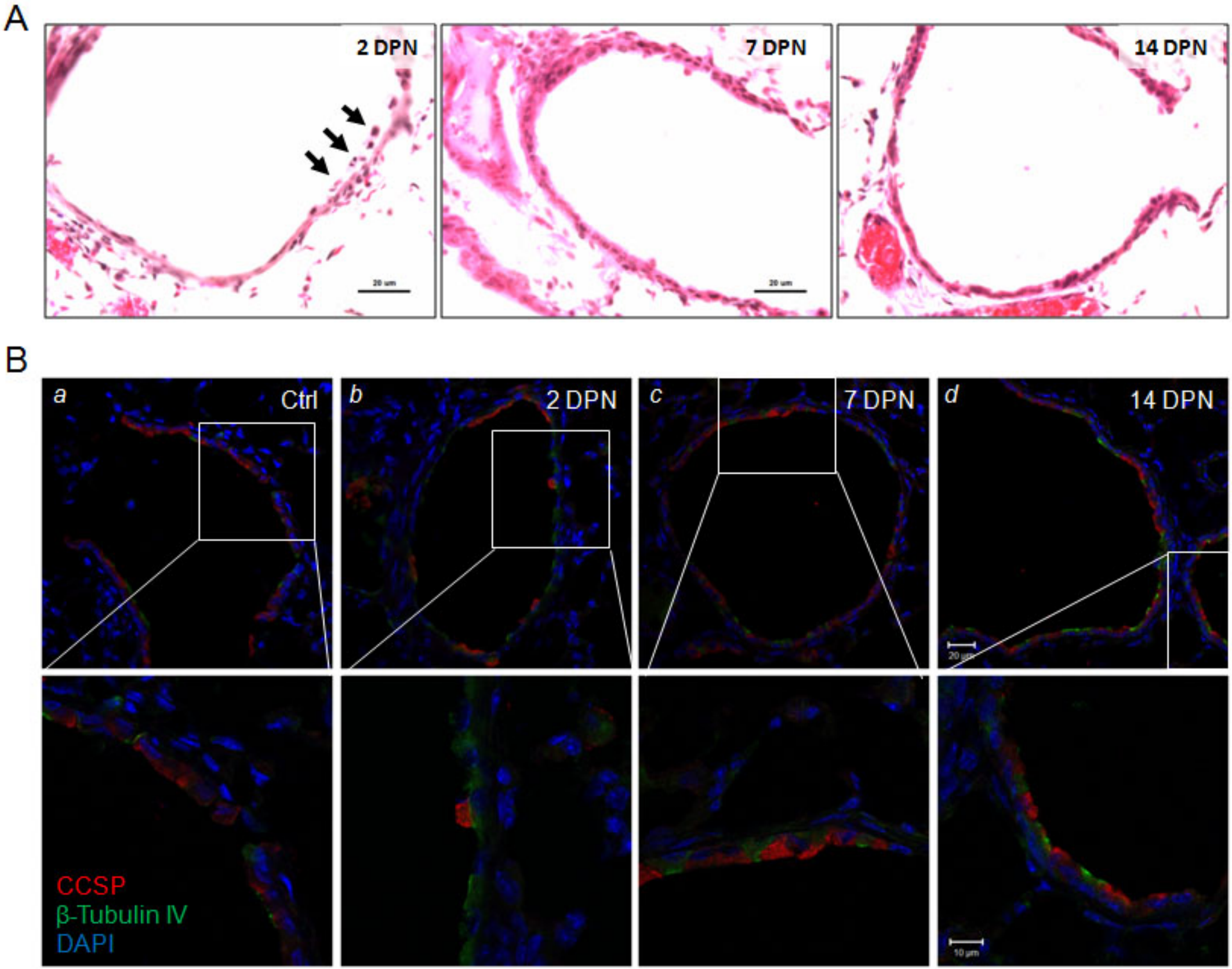
A
2 DPN
7 DPN
14 DPN
B
a
Ctrl
b
2 DPN
c
7 DPN
d
14 DPN
CCSP
β-Tubulin IV
DAPI